Nuclear Engineering and Technology 55 (2023) 1775–1782

Contents lists available at ScienceDirect

Nuclear Engineering and Technology

journal homepage: www.elsevier.com/locate/net

Evaluation of neutronics parameters during RSG-GAS commissioning by using Monte Carlo code

Surian Pinem [a, *], Wahid Luthfi [a], Peng Hong Liem [b, c], Donny Hartanto [d, 1]

[a] Research Center for Nuclear Reactor Technology, Research Organization for Nuclear Energy, National Research and Innovation Agency (BRIN), 80th Building of PUSPIPTEK Serpong, South Tangerang, Banten, Indonesia
[b] Cooperative Major in Nuclear Energy, Graduate School of Engineering, Tokyo City University (TCU), 1-28-1, Tamazutsumi, Setagaya, Tokyo, Japan
[c] Scientific Computational Division, Nippon Advanced Information Service, (NAIS Co., Inc.), 416 Muramatsu, Tokaimura, Ibaraki, Japan
[d] Oak Ridge National Laboratory One Bethel Valley Road, Oak Ridge, TN, 37830, USA

ARTICLE INFO

Article history:
Received 30 September 2022
Received in revised form
19 December 2022
Accepted 8 January 2023
Available online 16 January 2023

Keywords:
Neutronic parameter
Control rod worth
Fuel element reactivity
RSG-GAS
Serpent 2

ABSTRACT

Several reactor physics commissioning experiments were conducted to obtain the neutronic parameters at the beginning of the G.A. Siwabessy Multi-purpose Reactor (RSG-GAS) operation. These parameters are essential for the reactor to safety operate. Leveraging the experimental data, this study evaluated the calculated core reactivity, control rod reactivity worth, integral control rod reactivity curve, and fuel reactivity. Calculations were carried out with Serpent 2 code using the latest neutron cross-section data ENDF/B-VIII.0. The criticality calculations were carried out for the RSG-GAS first core up to the third core configuration, which has been done experimentally during these commissioning periods. The excess reactivity for the second and third cores showed a difference of 510.97 pcm and 253.23 pcm to the experiment data. The calculated integral reactivity of the control rod has an error of less than 1.0% compared to the experimental data. The calculated fuel reactivity value is consistent with the measured data, with a maximum error of 2.12%. Therefore, it can be concluded that the RSG-GAS reactor core model is in good agreement to reproduce excess reactivity, control rod worth, and fuel element reactivity.

1. Introduction

The G. A. Siwabessy Multi-purpose Reactor (RSG-GAS) is an open pool, water-cooled, and water-moderated reactor with a nominal power of 30 MW, which reached its first criticality in July 1987. The reactor core uses plate-type U_3O_8–Al fuel, which is later converted to U_3Si_2–Al fuel with the same uranium density of 2.96 g/cc and enriched at 19.75%. For a better neutron economy, beryllium is used as a reflector. The RSG-GAS typical working core configuration (TWC) consists of 40 fuel elements (FE), 8 control elements (CE), and 30 beryllium reflector elements. The TWC core was achieved through 5 transition cores with different amounts of fuel loading. The average thermal neutron flux is 2.0×10^{14} n/cm^{2}s, and its maximum neutron flux is at the center irradiation position (CIP), up to 5.38×10^{14} n/cm^{2}s. The RSG-GAS is equipped with several test facilities such as a CIP, 4 small irradiation positions (IP) in the reactor core, beam tubes for radioisotope production and basic science experiments, and power reactors fuel development such as power ramp test, fuel irradiation facilities, and others.

During the RSG-GAS commissioning period, experiments related to the reactor physics parameters have been carried out. These parameters are essential for the safety of reactor operation. With the availability of the commissioning experiment data, as well as the recent rapid development of high-fidelity reactor physics codes and nuclear data libraries, it is now possible to evaluate the reactor physics parameters with almost exact modeling of the experimented reactor conditions. It is worthily noted here that not only static experiments but whole core burnup analyses based on the detailed operation history (including control rod positions) are becoming realistic.

Reactivity is among these parameters, described as the departure from reactor criticality. Variations in absolute value, initiating event, and reactivity duration directly influence reactor safety operation, making reactivity one of the most important parameters related to reactor kinetics. The reactivity of the control rod depends on the position of the rod inside the core, the displacement of the control rod position, and its material composition [1,2]. For this reason, the measurement of control rod reactivity during the commissioning period of RSG-GAS first core was carried out by applying several methods such as rod drop, reactor period method, reactivity meter, and bank rod versus single rod compensation. All methods have their advantages and disadvantages. Based on the previous evaluation measured control rod reactivity in RSG-GAS first core, the compensation method is chosen to measure control rod reactivity [3].

* Corresponding author.
E-mail address: suri001@brin.go.id (S. Pinem).
[1] Work completed while employed at the University of Sharjah.

https://doi.org/10.1016/j.net.2023.01.008

The commissioning of the RSG-GAS provides a comprehensive range of experimental or measurement data for neutronics parameters with various core configurations and their corresponding control rod positions. These data can be used as benchmarking data to verify and validate the model of the reactor core. The criticality calculation and kinetic parameters of RSG-GAS first core have been carried out using various methods [4–10]. In this paper, we evaluate the excess reactivity, the control rod worth, the integral reactivity curve, and the reactivity of the fuel element. The results of this calculation could become good benchmark data for validating the calculation technique related to neutronics parameters in research reactors. The evaluation of neutronics parameters was carried out using the RSG-GAS second (transition) core because, in that core, most of the fuel elements from the first core were also being used besides several new fuel elements. The measurement data for neutronics parameters, i.e., the criticality, control rod worth, control rod reactivity curve, and fuel element reactivity value, are also available at the beginning of the cycle (BOC) and end of the cycle (EOC) conditions. The reactor was operated in one operating cycle from BOC to EOC for about 75.6 days (322,609 MWD). Calculations were performed using a continuous energy Monte Carlo Serpent 2 code [11,12] with the latest nuclear data library ENDF/B-VIII.0 [13]. The analyses are carried out according to the operation history of the particular core, and the calculated results are compared with the experimental data.

1.1. Transition core of RSG-GAS

The TWC core of the RSG-GAS is achieved after operating the reactor for 6 transition cores with a gradual increase in both the number of fuel elements and the reactor power [14]. The first core configuration consists of 12 fuel and 6 control rods with a maximum operating power of 10.6 MW. The second core configuration consists of 16 standard fuel elements, 6 control rods, and 58 beryllium blocks and achieves maximum power at 13.6 MW. The third RSG-GAS core consists of 22 fuel elements and 8 control rods with a maximum power of 18.19 MW.

The RSG-GAS fuel element is a material testing reactor (MTR) type fuel element with a standard fuel element consisting of 21 fuel plates, as shown in Fig. 1(a). Each fuel plate consists of an $AlMg_2$ frame and two cladding sheets with the same material enclosing U_3O_8–Al fuel meat. U_3O_8–Al is a uranium oxide fuel dispersed in an aluminum matrix, with 19.75% enriched uranium and 2.96 gU/cc uranium density. The active length of the fuel element is 60 cm, with nominal U-235 loading per standard fuel element being 250 g. The control fuel element is a fuel element designed to facilitate a fork-type neutron absorber containing an Ag–In–Cd, as shown in Fig. 1 (b). The control fuel element has 15 fuel plates to provide space for the control rod. A total of three fuel element plates were taken at each side of the fuel element, which made the nominal U-235 loading for the control fuel element 178.57 g. The primary data for the first to the third core for RSG-GAS are shown in Table 1, and the second core configuration is shown in Fig. 2.

Table 1
Main design data of RSG-GAS [14].

Parameters	First core	Second core	Third core
Nominal power (MWth)	10.6	13.60	18.19
No. of fuel elements	12	16	22
No. of control elements	6	6	8
No. of beryllium blocks	42	58	29
Fuel/control element dimension (mm)	77.1 × 81 × 600		
Fuel plate thickness (mm)	1.3		
Coolant channel width (mm)	2.55		
Number of plates per fuel element	21		
Number of plates per control element	15		
Fuel plate clad material	$AlMg_2$		
Fuel plate clad thickness (mm)	0.38		
Fuel plate dimension (mm)	0.54 × 62.75 × 600		
Fuel meat material	U_3O_8–Al		
U-235 enrichment (w/o)	19.75		
Uranium density in meat (g/cc)	2.96		
U-235 loading per fuel element (g)	250		
U-235 loading per control element (g)	178.6		
Absorber meat material	Ag–In–Cd		
Absorber thickness (mm)	3.38		
Absorber clad material	SS-321		

Beryllium is used as a reflector material surrounding the RSG-GAS core. Two rows of beryllium elements enclose the two sides of the reactor core to provide flexibility in adding desired irradiation kit. The beryllium elements consist of a lower end fitting, a rectangular beryllium rod with a height of 683 mm, and an outer cross-sectional dimension of 79 mm × 75 mm. Several beryllium elements are provided with one orifice with a diameter of 50 mm for the irradiated samples. The other two sides of the reactor core are connected to a beryllium reflector block specially designed to provide neutron beam

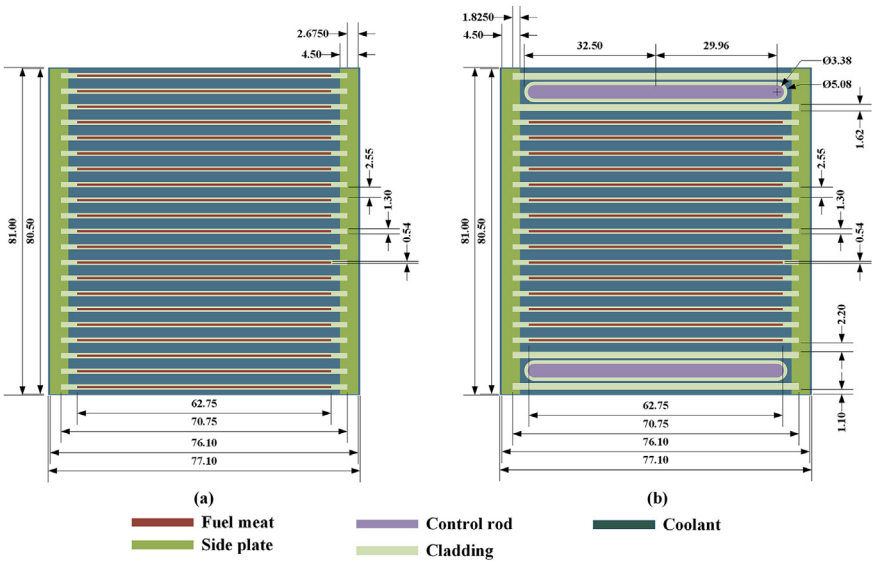

Fig. 1. Standard fuel element (a) and control element (b) layout (mm) [6].

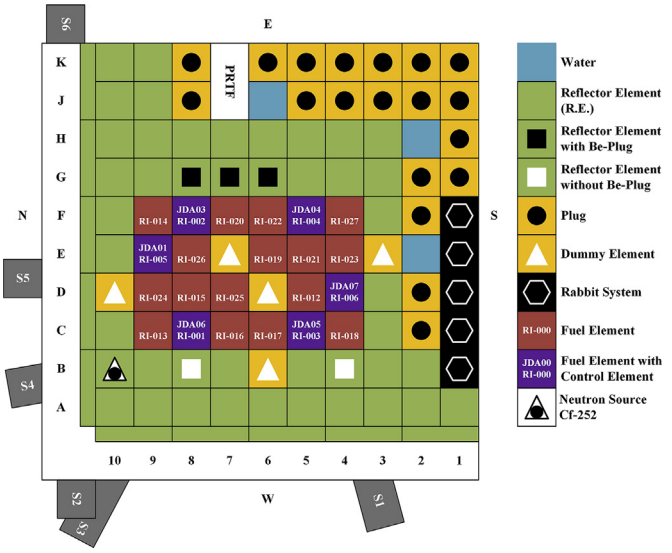

Fig. 2. RSG-GAS second core configuration [14].

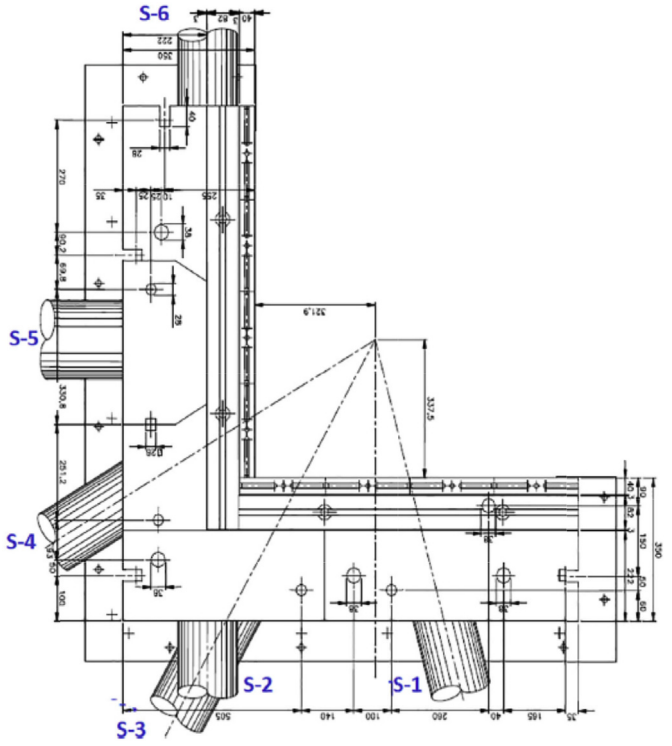

Fig. 3. Beryllium block reflector and beam tube of the RSG-GAS reactor (unit in mm) [14].

tubes. A configuration of 6 neutron beam tubes (S-1, S-2, S-3, S-4, S-5, and S-6) mounted on a beryllium block reflector is shown in Fig. 3.

2. Experiment method

2.1. Excess reactivity

Excess reactivity was measured after fuel elements were loaded and the reactor achieved criticality. This critical condition was the basis for determining excess reactivity caused by loading fuel and reflector elements. The RSG-GAS second core was critical with 11 fuel elements and 6 control rods, while the control rod bank was 600 mm and the regulating rod was 462 mm. After reaching the critical condition, excess reactivity measurement was carried out using the compensation method with a reactivity meter and control rod bank. Loading additional fuel elements for excess reactivity were added one by one with a total of 4 new fuel elements and 6 reflector elements at once. Reactivity measurement was conducted at each fuel loading and all six reflectors by measuring the control rod displacement using the compensation method. Core configuration after fuel loading for excess reactivity to RSG-GAS second core is shown in Fig. 2.

2.2. Control rod worth

The control rod worth was determined using a reactivity meter. Based on the point kinetic equation, the time-dependent reactivity $\rho(t)$ is defined as follows,

$$\rho(t) = \beta + \Lambda \frac{d}{dt}[lnP(t)] - \beta \int_0^\infty D(\tau)\frac{P(t-\tau)}{P(t)}d\tau$$

with

$$D(\tau) = \sum_j \frac{\beta_j \lambda_j}{\beta} e^{-\lambda_j \tau}$$

where $P(t)$ is time-dependent reactor power, β is the effective delayed neutron fraction, β_j is the jth group of delayed neutron fraction, λ_j is a decay constant of the jth group of delayed neutron precursors, and Λ is the effective neutron generation time. All quantities β, β_j, λ_j, and Λ were input data that have been determined from reactor vendor design data [3], while $P(t)$ was counted as the signal amplitude taken from the compensated ionization chamber (CIC) neutron detector (JKT04). The JKT04 is a detector connected to a reactivity meter.

Initially, the reactor was operated at source-free low power conditions so that it was free from neutron source effect and the reactivity feedbacks were negligible. The core temperature when measuring the reactivity of the control rods was 28 °C. The position of the control rods characterized source-free conditions that remain unchanged (the critical state) at different power levels.

Table 2
Control rod calibration position data of second core at BOC.

Calibrated control rod	Control rod position (mm)						Number of steps
	JDA01 /E-9	JDA03 /F-8	JDA04 /F-5	JDA05 /C-5	JDA06 /C-8	JDA07 /D-4	
JDA-01/E-9	**0–600**	320–525	320–525	320–525	320–525	320–525	20
JDA-03/F-8	289–206	**0–600**	289–206	289–206	289–206	289–206	24
JDA-04/F-5	290–184	290–184	**0–600**	290–184	290–184	290–184	28
JDA-05/C-5	279–221	279–221	279–221	**0–600**	279–221	279–221	19
JDA-06/C-8	323–239	323–239	323–239	323–239	**0–600**	323–239	23
JDA-07/D-4	277–223	277–223	277–223	277–223	277–223	**0–600**	18

Table 3
Control rod calibration position data of second core at EOC.

Calibrated control rod	Control rod position (mm)						Number of steps
	JDA01/E-9	JDA03/F-8	JDA04/F-5	JDA05/C-5	JDA06/C-8	JDA07/D-4	
JDA-01/E-9	**0–600**	366–294	366–294	366–294	366–294	366–294	20
JDA-03/F-8	378–290	**0–600**	378–290	378–290	378–290	378–290	21
JDA-04/F-5	378–279	378–279	**0–600**	378–279	378–279	378–279	25
JDA-05/C-5	362–298	362–298	362–298	**0–600**	362–298	362–298	18
JDA-06/C-8	386–285	386–285	386–285	386–285	**0–600**	386–285	21
JDA-07/D-4	358–299	358–299	358–299	358–299	358–299	**0–600**	16

Table 4
Control rod position when measuring fuel element reactivity at BOC.

Fuel element	Core position	Control rod position (mm)	
		Bank	Regulating rod
Full core	–	253	253
RI-13-out	C-9	286	237
RI-14-out	F-9	286	286
RI-15-out	D-8	286	543
RI-18-out	C-4	286	242
RI-19-out	E–6	347	347
RI-24-out	D-9	286	321
RI-25-out	D-7	345	345
RI-27-out	F-4	286	278

During the control rod calibration, the control rod banks were in critical positions while the single control rod to be calibrated was withdrawn. After waiting for about 10 s to ensure the transient event caused by the calibrated control rod insertion was done, the bank rods were changed to compensate for the positive reactivity and brought the reactor to a critical state again. Each step of control rod calibration produced a reactivity value of about 10–20 cents. This procedure was repeated until the whole part of the control rod was calibrated. The accumulation of measured reactivity for each step of control rod compensation is the control rod's worth. Control rod positions and their corresponding bank rod positions are shown in Tables 2 and 3 for the second core configuration at the beginning of cycle (BOC) and end of cycle (EOC), respectively.

2.3. Fuel element reactivity

Measuring reactivity of fuel element was also done while the reactor was operated at the source-free low power. The reactivity measurement was carried out by removing each fuel from the core. The control rod was then positioned to bring the reactor back to critical condition; this position was then recorded. After the measurement is complete, the corresponding fuel is returned to its original position, so the measured fuel element is the only fuel outside the core while the measurement incur. The difference in control rod position determined the fuel element reactivity worth when the measured fuel was in and outside the core. The control rod position corresponded to fuel reactivity measurement at the BOC and EOC of the second core configuration, shown in Tables 4 and 5. The reactivity of each fuel element was determined by fitting the control rod position to the previously measured integral reactivity curve of the control rod.

Table 5
Control rod position when measuring fuel element reactivity at EOC.

Fuel element	Core position	Control rod position (mm)	
		Bank	Regulating rod
Full core	–	321	323
RI-12-out	D-5	391	391
RI-13-out	C-9	365	363
RI-14-out	F-9	362	366
RI-15-out	D-8	385	385
RI-16-out	C-7	380	390
RI-17-out	C-6	385	395
RI-18-out	C-4	353	352
RI-19-out	E–6	433	429
RI-20-out	F-7	409	406
RI-21-out	E–5	385	392
RI-22-out	F-6	396	394
RI-23-out	E–4	362	360
RI-24-out	D-9	365	361
RI-25-out	D-7	430	418
RI-26-out	E–8	400	401
RI-27-out	F-4	360	357

3. Calculation method

The first core of the RSG-GAS model from the previous study was used [10]. The depletion calculation by Serpent 2 code with ENDF/B-VIII.0 nuclear data was carried out using 50,000 neutron histories per cycle, and the total number of cycles was 200 with 50 inactive cycles, providing the standard deviation of the effective multiplication factor (k_{eff}) about 30–40 pcm. In addition, for the control rod worth calculations, the neutron histories per cycle were increased to 400,000 neutrons, and the total number of cycles is 500 with 100 inactive cycles to reduce the statistical uncertainty. The thermal scattering libraries S(α,β) for hydrogen in the light water and beryllium as metal were included in the calculations. Each fuel element was divided into five axial zones, and the material for each zone was defined separately. In total, 90 depletion zones were considered. The Serpent core model shown in Fig. 4.

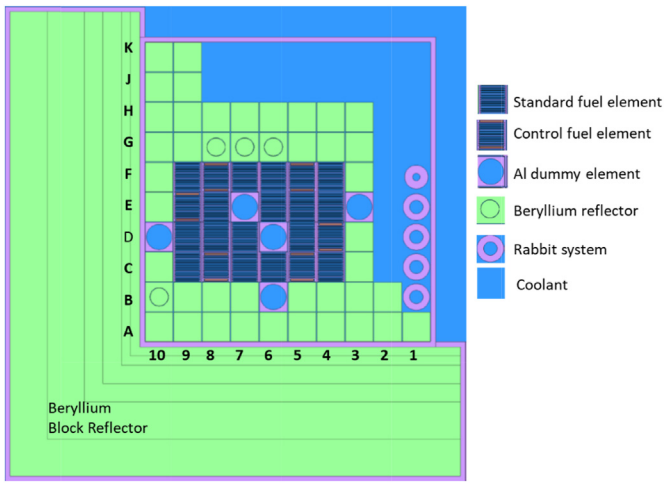

Fig. 4. Second working core configuration of RSG-GAS.

Table 6
Measured and calculated excess reactivity and control rod worth.

Parameters	2nd Core		3rd core	
	Experiment	Serpent 2	Experiment	Serpent 2
Excess reactivity (%)	9.48 ± 0.02	10.03 ± 0.001 (5.8%)	9.31 ± 0.01	9.57 ± 0.01 (2.7%)
Control rod worth (%)	−18.12 ± 0.043	−17.77 ± 0.009 (−1.9%)	−20.10 ± 0.040	−19.16 ± 0.01 (−4.7%)

Table 7
Control rod reactivity worth at BOC.

Control Rod	Reactivity control rod at BOC condition ($)	
	Experiment	Serpent 2
JDA01	3.660 ± 0.29	3.665 ± 0.14 (0.13%)
JDA03	4.475 ± 0.32	4.466 ± 0.21 (−0.21%)
JDA04	5.328 ± 0.34	5.357 ± 0.55 (0.55%)
JDA05	3.345 ± 0.29	3.374 ± 0.86 (0.87%)
JDA06	4.315 ± 0.31	4.358 ± 0.99 (0.99%)
JDA07	3.170 ± 0.28	3.171 ± 0.02 (0.02%)

4. Result and discussion

4.1. Core excess reactivity

Excess reactivity at BOC is evaluated by calculating the k_{eff}. The calculated result of the excess reactivity and control rods worth of the second core and third core are shown in Table 6. The deviation between Serpent 2 and experiment data is formulated as follows,

$$\left(\frac{Serpent\ 2}{Experiment} - 1\right) \times 100\%$$

The deviation in excess reactivity between calculated and experiment values for the second core was 5.8% (510.97 pcm), and the third core was 2.7% (253.23 pcm). The calculated values are considered in good agreement with the experiment data since the calculations also involved the whole core burnup calculations of the first and second cores. For the control rod worth, the Serpent 2 values show an underestimation slightly. The highest deviation was found for the third core, i.e., around 4.7%. Considering the measurement errors and the rod interaction effects, the Serpent 2 values agreed with the experiment data.

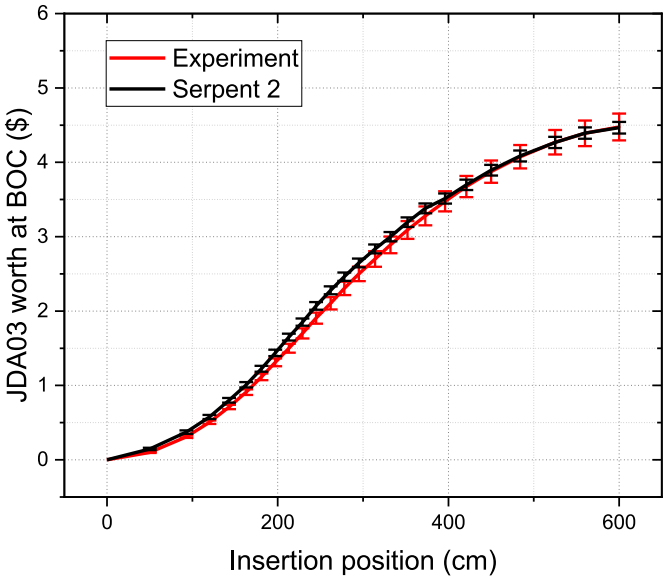

Fig. 6. JDA03 integral control rod worth curve at BOC.

4.2. Control rod worth

The measured and calculated results of the control rod worth for the second core at BOC are shown in Table 7. The difference between a calculation and measurement peaked at 0.99% for the JDA06 rod. These results indicate that the control rod worth based on Serpent 2 calculations is within good agreement with the experiment.

The calculated and measured integral control rod worth curve (S curve) at BOC for the second core is shown in Figs. 5–10. The compensation method explained before determined the integral control rod curve by calculating the reactivity derived from the k_{eff} values corresponding to the control rod positions. The Serpent 2

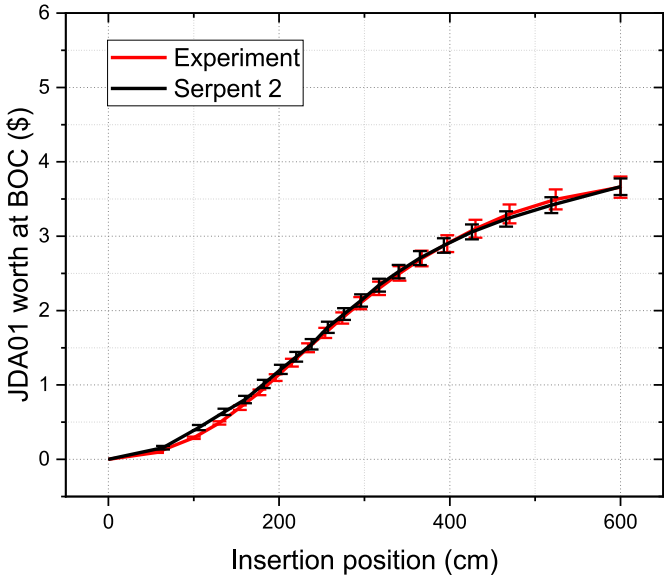

Fig. 5. JDA01 integral control rod worth curve at BOC.

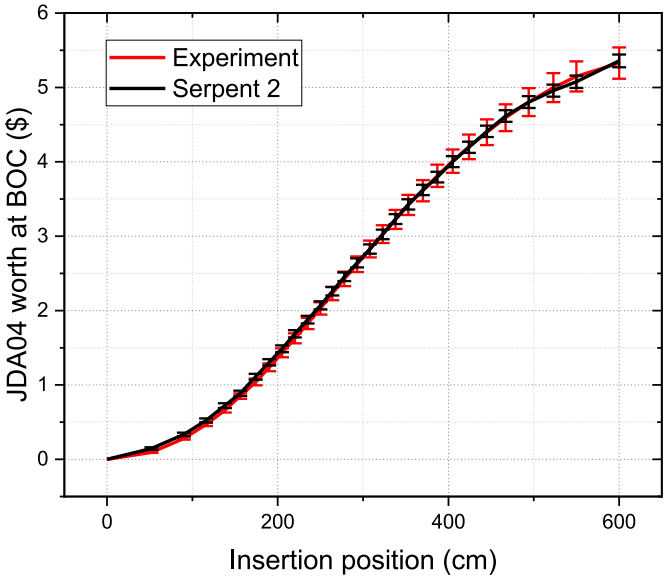

Fig. 7. JDA04 integral control rod worth curve at BOC.

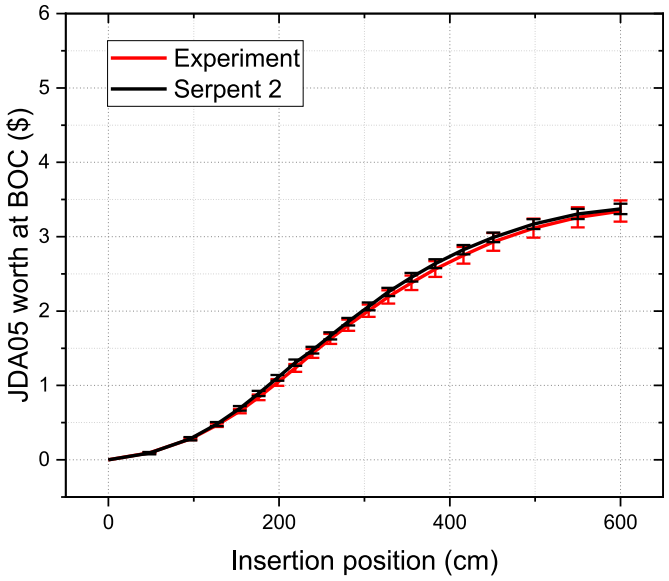

Fig. 8. JDA05 integral control rod worth curve at BOC.

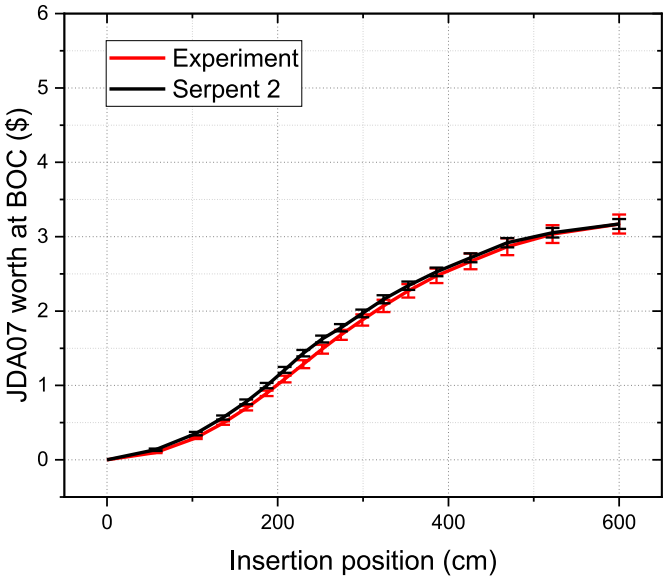

Fig. 10. JDA07 integral control rod worth curve at BOC.

calculated results of integral control rod worth were again within the range of measured data.

At the EOC of the second core, the control rod calibration was also carried out. The measured and calculated control rod worth at EOC are shown in Table 8. The maximum difference between the calculated and measured data at EOC was 0.78%, comparable to the BOC. The integral control rod worth of each control rod was also calculated and shown in Figs. 11–16 with its corresponding measured data. The most significant difference between calculations and measured data occurred in the JDA07 rod but was still within the measurement uncertainty range.

Table 8
Control rod reactivity worth at EOC.

Control Rod	Reactivity control rod at EOC condition ($)	
	Experiment	Serpent 2
JDA01	3.390 ± 0.29	3.405 ± 0.44 (0.44%)
JDA03	4.050 ± 0.31	4.052 ± 0.04 (0.04%)
JDA04	4.710 ± 0.32	4.681 ± 0.61 (−0.61%)
JDA05	3.270 ± 0.29	3.244 ± 0.78 (−0.78%)
JDA06	4.027 ± 0.31	4.051 ± 0.58 (0.58%)
JDA07	2.920 ± 0.26	2.938 ± 0.60 (0.60%)

4.3. Fuel element reactivity

The fuel element reactivity worth is determined based on the control rod position and compared to the control rod's integral control rod curve (S curve). The control rod S curve was obtained before the fuel reactivity measurement was carried out during the experiment. The calculation of fuel element reactivity with Serpent 2 was carried out by simulating the control rod position as the experiment occurred. Fuel element reactivity worth is then calculated according to the measured core reactivity (experimental) or

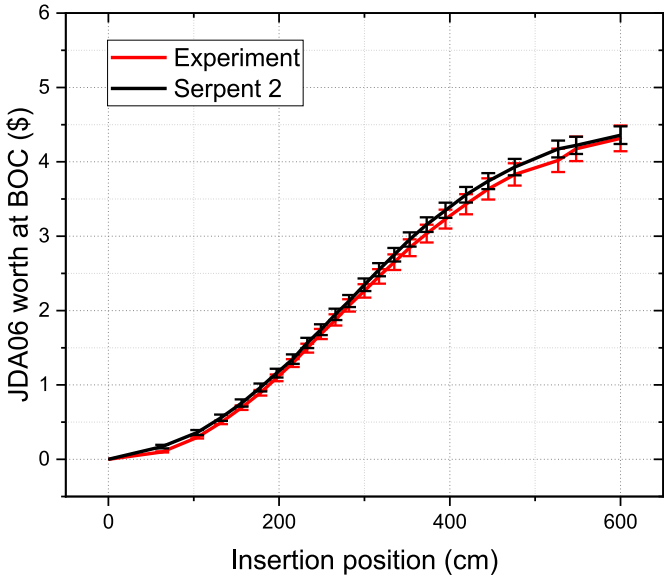

Fig. 9. JDA06 integral control rod worth curve at BOC.

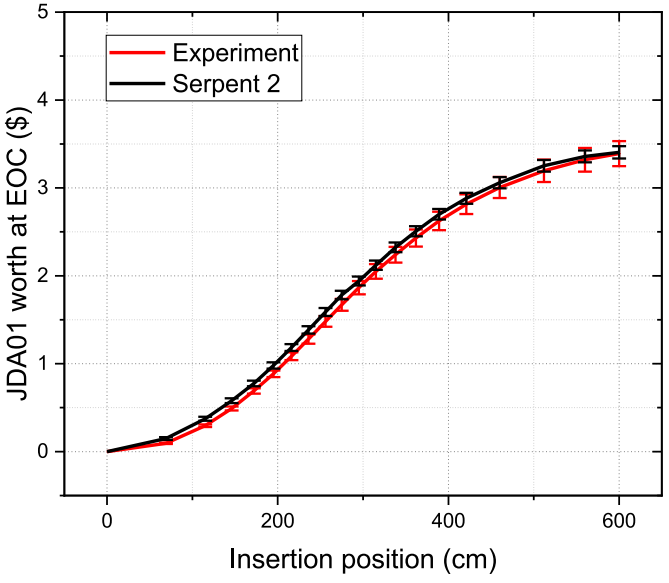

Fig. 11. JDA01 integral control rod worth curve at EOC.

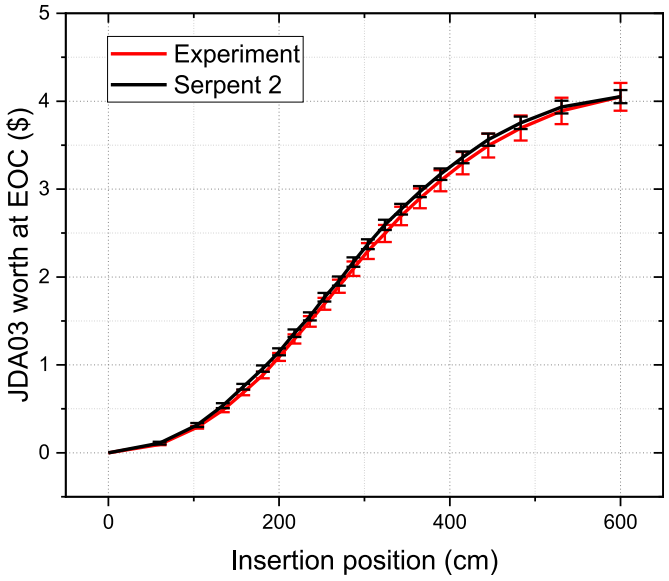

Fig. 12. JDA03 integral control rod worth curve at EOC.

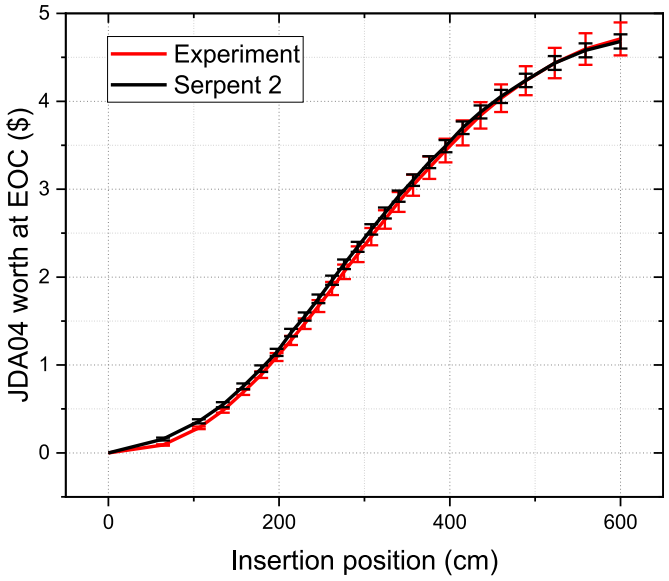

Fig. 13. JDA04 integral control rod worth curve at EOC.

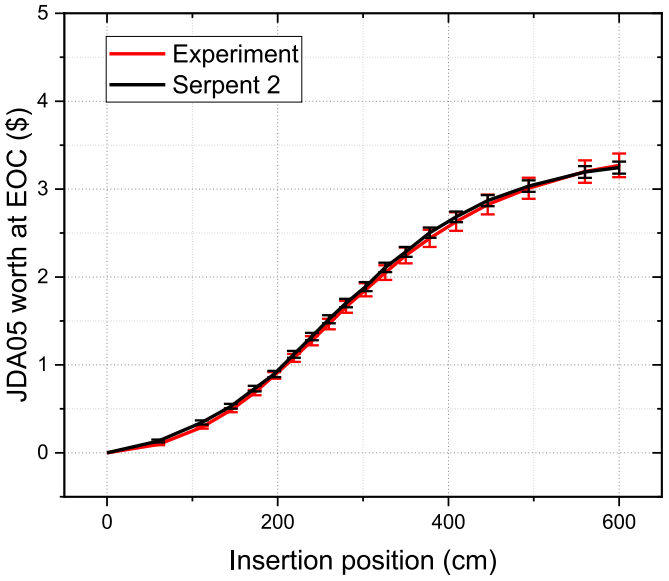

Fig. 14. JDA05 integral control rod worth curve at EOC.

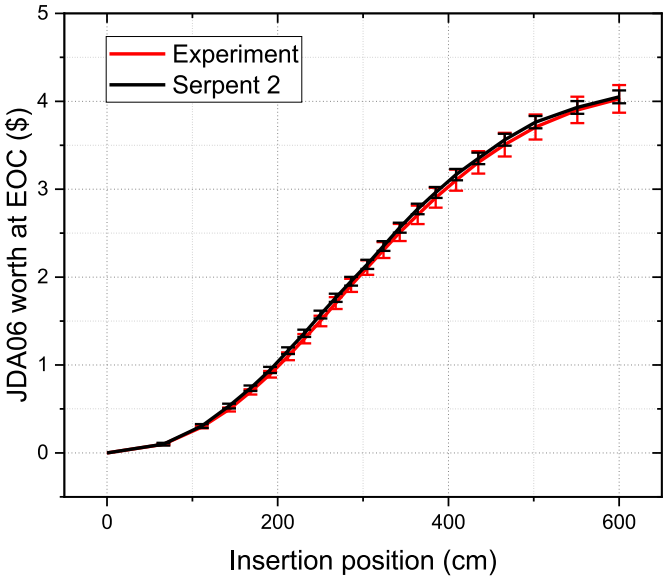

Fig. 15. JDA06 integral control rod worth curve at EOC.

the k_{eff} (calculation) when the fuel element is inside and outside the core.

The calculated results for fuel element reactivity at BOC and EOC are shown in Tables 9 and 10. For the second core BOC, Serpent 2 results were very close to the measured data with a maximum deviation of 1.82%. Meanwhile, the maximum deviation for the second core EOC was around 2.12%. The primary source of errors that might contribute to the uncertainty of the fuel reactivity measurement was related to the control rod position uncertainty, which was estimated to be ±1 mm. From the calibrated S curve of all 6 control rods, a 1 mm change of control rod position equals a reactivity value of about 4.09 cents.

5. Conclusions

Neutronics parameter analysis is essential to ensure a safe reactor operation. The analyses related to core excess reactivity, control rod worth, and fuel element reactivity have been carried out using the continuous energy Monte Carlo Serpent 2 code with the ENDF/B-VIII.0 nuclear data. The difference between the calculation and measurement of the excess reactivity for the RSG-GAS second and third cores was around 672 pcm and 511 pcm, respectively. The calculated integral control rod reactivity curves obtained by the bank rod compensation method were within the uncertainty range of measured data. The maximum difference in control rod worth at the RSG-GAS second core BOC and EOC is less than 1%. The calculated fuel element reactivity showed a maximum deviation of around 2% compared to the measured data. Overall, it can be concluded that the calculated neutronics parameters agree well with the measured commissioning data accumulated for the RSG-GAS second core.

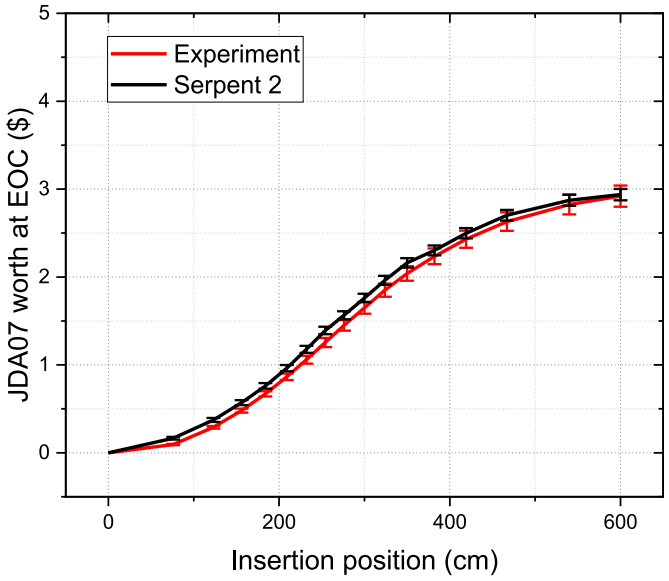

Fig. 16. JDA07 integral control rod worth curve at EOC.

Table 9
Fuel element reactivity worth at BOC.

Fuel element	Core position	Reactivity (cent)		Different (%)
		Experiment	Serpent 2	
RI-13	C-9	161.85	160.35 ± 2.27	−0.92
RI-14	F-9	219.50	218.90 ± 1.95	−0.27
RI-15	D-8	429.10	421.30 ± 2.01	−1.82
RI-18	C-4	167.67	166.20 ± 1.60	−0.88
RI-19	E-6	579.19	573.81 ± 2.05	−0.93
RI-24	D-9	248.26	249.09 ± 2.20	0.33
RI-25	D-7	568.36	563.20 ± 1.61	−0.91
RI-27	F-4	207.35	206.62 ± 1.72	−0.35

Table 10
Fuel element reactivity worth at EOC.

Fuel element	Core position	Reactivity (cent)		Different (%)
		Experiment	Serpent 2	
RI-12	D-5	363.11	357.14 ± 1.87	−1.64
RI-13	C-9	175.24	173.08 ± 1.73	−1.23
RI-14	F-9	226.89	223.98 ± 1.98	−1.28
RI-15	D-8	335.55	330.26 ± 1.65	−1.58
RI-16	C-7	320.89	316.23 ± 1.89	−1.45
RI-17	C-6	344.26	339.05 ± 1.99	−1.51
RI-18	C-4	194.49	192.23 ± 1.69	−1.16
RI-19	E-6	532.04	520.76 ± 2.02	−2.12
RI-20	F-7	438.82	430.65 ± 2.21	−1.86
RI-21	E-5	341.68	336.45 ± 2.20	−1.53
RI-22	F-6	383.79	377.21 ± 1.60	−1.71
RI-23	E-4	221.16	218.21 ± 1.95	−1.34
RI-24	D-9	234.54	231.29 ± 1.60	−1.39
RI-25	D-7	514.84	503.92 ± 2.22	−2.12
RI-26	E-8	403.86	396.84 ± 1.69	−1.74
RI-27	F-4	209.90	207.12 ± 1.82	−1.32

Credit authorship contribution statement

Surian **Pinem:** Conceptualization, Validation, Formal Analysis, Writing Original Draft, Review & Editing. **Wahid Luthfi:** Data Curation, Visualization, Writing Original Draft, Review & Editing. **Peng Hong Liem:** Conceptualization, Software, Writing Original Draft, Review & Editing. **Donny Hartanto:** Data Curation, Methodology, Review & Editing.

Declaration of competing interest

The authors declare that they have no known competing financial interests or personal relationships that could have appeared to influence the work reported in this paper.

Acknowledgments

The authors are very grateful to the RSG-GAS multipurpose reactor staff members for conducting the experiments. This research was supported by the Indonesian government through DIPA for the 2021 fiscal year funding number SP DIPA-080.01.1.450310/2021.

References

[1] Q.B. Do, G.T. Phan, K.C. Nguyen, Q.H. Ngo, H.N. Tran, Criticality and rod worth analysis of the DNRR research reactor using the SRAC and MCNP5 codes, Nucl. Eng. Des. 343 (2019) 197–209, https://doi.org/10.1016/j.nucengdes.2019.01.011.
[2] P. Kaviani, J. Mokhtari, S.M. Mirvakili, Integral form of the control rod calibration curve in the new core configuration of HWZPR using rod insertion method, Prog. Nucl. Energy 125 (2020), 103375, https://doi.org/10.1016/j.pnucene.2020.103375.
[3] PRSG, Report of the Operation of RSG-GAS Reactor First Core, vol. 60, National Nuclear Energy Agency of Indonesia, Serpong, Indonesia, 1988.
[4] L.P. Hong, Monte Carlo calculations on the first criticality of the multipurpose reactor GA Siwabessy, At. Indones. 24 (2) (1998).
[5] T.M. Sembiring, S. Pinem, Validation of the Monte Carlo code MVP on the first criticality of Indonesian multipurpose reactor, in: Proceedings of International Conference on Research Reactors, Safe management and effective utilization, Sydney, Australia, 2007, pp. 5–9 (Nov).
[6] P.H. Liem, T.M. Sembiring, Benchmarking the new JENDL-4.0 library on criticality experiments of a research reactor with oxide LEU (20 w/o) fuel, light water moderator and beryllium reflectors, Ann. Nucl. Energy 44 (2012) 58–64, https://doi.org/10.1016/j.anucene.2012.01.017.
[7] T.M. Sembiring, P.H. Liem, Accuracy of the ENDF/B-VII. 0 nuclear data library on the first criticality experiments of the Indonesian multipurpose reactor RSG GAS, in: Proceedings of the 2013 International Conference on Nuclear Data for Science and Technology, 2013, pp. 4–8. ND2013.
[8] P.H. Liem, T. Surbakti, D. Hartanto, Kinetics parameters evaluation on the first core of the RSG GAS (MPR-30) using continuous energy Monte Carlo method, Prog. Nucl. Energy 109 (2018) 196–203, https://doi.org/10.1016/j.pnucene.2018.08.014.
[9] P.H. Liem, D. Hartanto, Sensitivity and uncertainty analysis on the first core criticality of the RSG GAS multipurpose research reactor, Prog. Nucl. Energy 114 (2019) 46–60, https://doi.org/10.1016/j.pnucene.2019.03.001.
[10] D. Hartanto, P.H. Liem, Analysis of the first core of the Indonesian multipurpose research reactor RSG-GAS using the Serpent Monte Carlo code and the ENDF/B-VIII. 0 nuclear data library, Nucl. Eng. Technol. 52 (12) (2020) 2725–2732, https://doi.org/10.1016/j.net.2020.05.027.
[11] J. Leppänen, M. Pusa, T. Viitanen, V. Valtavirta, T. Kaltiaisenaho, The Serpent Monte Carlo code: status, development and applications in 2013, Ann. Nucl. Energy 82 (2015) 142–150, https://doi.org/10.1016/j.anucene.2014.08.024.
[12] Alberto Talamo, Yan Cao, Yousry Gohar, V. Valtavirta, J. Leppänen, S. Sikorin, S. Mandzik, S. Polazau, T. Hryharovich, Serpent transient analyses of GIACINT geometrical change experiments, Ann. Nucl. Energy 64 (2021) 1–30, https://doi.org/10.1016/j.anucene.2021.108601.
[13] D.A. Brown, M.B. Chadwick, R. Capote, A.C. Kahler, A. Trkov, M.W. Herman, et al., ENDF/B-VIII. 0: the 8th major release of the nuclear reaction data library with CIELO-project cross sections, new standards and thermal scattering data, Nucl. Data Sheets 148 (2018) 1–142, https://doi.org/10.1016/j.nds.2018.02.001.
[14] U. Jujuratisbela, B. Arbie, S. Pinem, L. Suparlina, O.P. Singh, Kinetics parameter measurements on RSG-GAS, a low-enriched fuel reactor, in: Proceedings of XIV International Conference on Reduced Enrichment for Research and Test Reactor, 1991. Jakarta, Indonesia, 4-7 Nov, https://inis.iaea.org/collection/NCLCollectionStore/_Public/35/047/35047142.pdf.